AIAA 82-4064

Combustion Properties of Carbon Slurry Drops

G. A. Szekely Jr.* and G. M. Faeth†
The Pennsylvania State University, University Park, Pa.

A theoretical and experimental investigation of the combustion properties of carbon slurry fuels is described. The combustion of individual drops (400-1000 μm in diameter) supported at various positions within an open turbulent diffusion flame was observed. When a slurry drop was exposed to the flame, the liquid fuel evaporated in the first stage of the process leaving a porous carbon agglomerate formed from the carbon particles in the slurry. The second stage involved heat-up and reaction or quenching of the agglomerate. Consumption of the agglomerate was the slowest step in the process, requiring 90-95% of the drop lifetime, even in regions where maximum agglomerate reaction rates were observed. An analysis was developed to provide predictions of both liquid and agglomerate heat-up and gasification. The analysis yielded good predictions of both particle size and temperature variations for flame equivalence ratios of 0.272-1.350. The use of a catalyzed slurry was found to increase agglomerate burning rates in the lean portions of the flame, extending the lean limit of agglomerate reaction.

Nomenclature

a_i = area/reactivity factor
A_i = pre-exponential factor
C_p = specific heat
d = flame jet diameter
d_p = particle diameter
D = effective binary diffusivity
E_i = activation energy
i = enthalpy
i_f = enthalpy of formation
K = dimensionless mass burning rate, Eq. (15)
K_{pi} = equilibrium constant
K_{ri} = reaction rate constant
Le = Lewis number
m_i, m = mass of species i in particle and total particle mass
$\dot{m}_i'', \dot{m}''$ = mass flux of species i and net mass flux
M_i, M = molecular weight of species i and mixture
n_i = reaction order
Nu, Nu' = Nusselt number, Eqs. (10) and (12)
p_i, p = partial pressure of species i and total pressure
Pr = Prandtl number
q_c'', q_r'' = convective and radiative heat flux at particle surface
r = radial distance
R = Universal gas constant
Re = Reynolds number
R_i = reaction rate of species i
Sc = Schmidt number
Sh, Sh' = Sherwood number, Eqs. (10) and (12)
t = time
T = temperature
u = gas velocity relative to particle
x = distance from exit of flame jet
$Y_i, \tilde{Y}_i$ = mass fractions of species and element i
ϵ = surface emissivity
ζ = convective enhancement factor
λ = thermal conductivity
μ_{ij} = stoichiometry parameters, Eq. (2)
ν = kinematic viscosity
ρ = density
σ = Stefan-Boltzmann constant
ϕ = equivalence ratio
χ = reaction parameter, Eq. (20)

Subscripts

avg = average condition
c = carbon
f = liquid
p = particle surface
ref = reference condition
w = surface of enclosure
0 = initial condition
∞ = surroundings of particle

Received April 16, 1981; revision received Aug. 24, 1981.

*Research Assistant, Dept. of Mechanical Engineering and The Applied Research Laboratory.

†Professor, Dept. of Mechanical Engineering and The Applied Research Laboratory. Member AIAA.

Introduction

LIQUID fuels having high-energy densities are of interest in order to improve the performance of volume-limited propulsion systems.[1] It has become increasingly difficult, however, to obtain additional improvements employing liquids alone.[2] Therefore, slurries are increasingly receiving attention since they can be handled and burned similar to liquids, but have higher energy densities due to the presence of solids.[2-4]

The objective of the present investigation was to examine the combustion properties of a particular class of slurry fuels, namely, slurries employing carbon black particles as the solid phase. The general combustion properties of similar carbon slurries have been examined in gas turbine combustors[2,3] and in well-stirred reactors.[4] The present study emphasized more fundamental aspects of the problem by observing and analyzing the combustion properties of individual slurry drops.

Coal slurries have received attention in recent years since their use provides a means of extending limited petroleum reserves. While the presence of ash and volatile material in coal modifies the combustion process in comparison to carbon slurries, past observations of coal slurry combustion provide useful background information for the present investigation. The results of Law and co-workers,[5,6] for both supported and freely falling coal slurry drops burning in air, are representative of recent findings in this area. A two-stage combustion process was observed. The liquid fuel evaporated or burned in the first stage, leaving an irregular agglomerate of the coal particles in the slurry. The second stage involved heat-up and reaction or quenching of the agglomerate. Even for conditions where reaction of the agglomerate was observed, this stage of the process was relatively slow, comprising the bulk of the lifetime of the slurry drop.

During the present investigation, the combustion of carbon slurry drops was observed using the supported drop technique

Table 1 Summary of flame properties at droplet test locations[a]

				Mass fractions				
x/d	T, K	u, m/s	ϕ	O_2	CO_2	CO	N_2	H_2O
170.0	1841	9.93	1.350	0.006	0.101	0.079	0.653	0.161
212.5	1903	8.14	0.939	0.021	0.094	0.051	0.689	0.145
255.0	1824	6.15	0.870	0.076	0.079	0.039	0.677	0.129
297.5	1541	4.82	0.761	0.093	0.075	0.031	0.688	0.113
340.0	1271	4.35	0.557	0.122	0.066	0.016	0.699	0.097
382.5	1101	4.21	0.484	0.136	0.057	0.013	0.705	0.089
467.5	887	3.90	0.348	0.163	0.038	0.007	0.717	0.075
510.0	779	2.93	0.272	0.176	0.029	0.004	0.724	0.067

[a] Mean conditions along the centerline of a burning vertical propane jet with a visible flame height of 460 mm. The jet exit diameter and velocity were 1.194 mm and 88.7 m/s, yielding a Reynolds number of 23,600. Ambient conditions were still air at 296 ± 3 K at 97 kPa.

(drop diameters in the 400-1000 μm range). In order to approximate combustion chamber conditions, the drops were supported at various positions within an open turbulent diffusion flame at atmospheric pressure. The measurements yielded the variation of particle size and temperature as a function of time. Carbon agglomerates were observed during the tests and their surface structure was examined using a scanning electron microscope (SEM). An analysis was developed to provide predictions of both liquid and agglomerate heat-up and gasification. The analysis was evaluated using measurements for flame equivalence ratios of 0.272-1.350. The effect of a catalyst on agglomerate combustion properties was also considered.

Experimental Methods

Test Apparatus

The slurry drops were supported along the centerline of an open turbulent diffusion flame that had been studied earlier.[7] The arrangement consisted of a combusting propane jet directed vertically upward with the propane flame stabilized at the jet exit using an array of small hydrogen capillary flames. A single operating condition was employed for all tests. The test droplets were located at various positions along the centerline of the flame. Flow properties at each drop location considered during this investigation are summarized in Table 1. These properties were determined by measuring velocities with a laser-Doppler anemometer, temperatures with a 50 μm diam thermocouple and concentrations by isokinetic sampling and gas chromatography.

The fuel drops were mounted on either the bead of a thermocouple junction or a quartz fiber. The drops were mounted with a hypodermic needle, while the flame was deflected from the test position. The combustion process was initiated by retracting the deflector with a pneumatic cylinder.

Instrumentation

The drops were observed as shadowgraphs with a 16-mm motion picture camera operating at speeds of 50-100 frames/s. The film speed was monitored with 10-ms timing marks. The camera optics provided a 2:1 magnification. The drops were blacklighted with a collimated beam from a mercury arc lamp. The films were analyzed on a Vanguard motion picture analyzer. The particles were not always spherical in shape; therefore, an equivalent diameter is reported for a sphere having the same volume as the ellipsoidal-shaped particles.[8]

Particle temperatures were measured by mounting the drops on the junction of a Pt/Pt 10% Rh thermocouple constructed of 75 μm diam wires. To help support the drop, the junction was placed within a spherical Sauereisen cement bead (300-400 μm in diameter). The thermocouple output was recorded digitally on a Nicolet Explorer Oscilloscope, Model 206.

Samples of the carbon agglomerates were obtained after quenching the process by redeflecting the flame. These samples were studied using a scanning electron microscope (International Scientific Instruments, Model M-7).

Test Fuels

Two slurry fuels provided by Suntech Group were examined during the tests. The fuels consisted of a medium thermal carbon black having an ultimate particle size of 0.3 μm, with JP-10 as the liquid fuel (see Ref. 2 for more complete specifications). The bulk of the testing was conducted with a noncatalyzed slurry having 50.4% dispersed carbon by weight. A catalyzed slurry that had 49.2% dispersed carbon by weight and contained a proprietary lead compound as a catalyst was also considered. While these fuels are representative carbon slurries, fuel development efforts are continuing and they do not necessarily represent the most attractive formulations.

Liquid Gasification Theory

The measurements suggested that the life history of a slurry drop could be divided into two separate phases—liquid heat-up and evaporation followed by agglomerate heat-up and reaction; therefore, the analysis was separated in the same manner. The objective of both phases of the analysis was to predict the particle life history, i.e., the variation of particle temperature, mass, and diameter as a function of time.

The following assumptions were adopted for both phases of the analysis:

1) Spherical particles with no particle interaction were considered, in order to correspond with present test conditions.

2) The flowfield around the particle was assumed to be quasisteady, i.e., at each instant of time the flow is equivalent to a steady flow for the same boundary conditions and the velocity of the surface was neglected. Ambient properties were taken to be local mean properties.

3) Exact treatment of flow around spheres is not practical for use in spray models; therefore, the conventional film theory approximations were employed to treat convection.[8] This implies that gas-phase transport can be represented as a stagnant, spherically symmetric layer whose outer radius is determined from empirical convection correlations for spheres.

4) Only diffusion of mass by concentration gradients was considered, employing an effective binary diffusivity. All species were assumed to have equal molecular weights and specific heats, and constant average gas-phase properties were employed at each instant of time. Average properties were computed at a mean state, defined as:

$$\phi_{\text{avg}} = \alpha\phi_p + (1-\alpha)\phi_\infty \tag{1}$$

where ϕ represents both temperature and species mass fractions. Predictions vary significantly as α is changed; a single value was chosen to provide best agreement between predictions and measurements over the test range. Methods developed during past work were employed to compute properties.[7-10]

5) Particle properties were assumed to be uniform at each instant of time.

In addition, the following assumptions were specifically adopted for the liquid phase portion of the analysis: the liquid was assumed to evaporate with no envelope flame present, since envelope flames were not observed at the test conditions considered here; radiation was ignored; the liquid surface was assumed to be in thermodynamic equilibrium with the vapor pressure curve yielding the relationship between surface temperature and vapor concentration; and the solubility of gases in the liquid was assumed to be negligible.

These assumptions are generally similar to those employed for drop transport analyses near atmospheric pressure and a further discussion of their justification can be found in Ref. 11. The resulting formulation and method of solution are identical to that employed by Mao et al.,[10] except that the heat capacity and volume of the particle must include the effect of the carbon particles, $mC_p = m_f C_{pf} + m_c C_{pc}$ and $\pi d_p^3/6 = m_f/\rho_f + m_c/\rho_c$ where ρ_c for the present carbon black agglomerates was obtained from Bruce et al.[2,3]

The liquid gasification theory was checked by comparing predicted and measured life histories for pure JP-10 drops at various positions in the flame. Similar to earlier experience in this laboratory,[7-10] good agreement between predictions and measurements was obtained using $\alpha = 0.9$. The dominance of properties near the drop surface is reasonable, since mass transfer rates are high in a flame environment, resulting in a substantial blowing effect in the gas phase.

Agglomerate Reaction Theory

Analysis of the agglomerate phase of the process follows the approach developed in recent studies of carbon particle combustion,[12,13] but differs in some details. In addition to the five assumptions discussed earlier, the following assumptions were adopted:

6) The particle was pure carbon while the gas mixture in the flow was approximated by O_2, N_2, CO_2, CO, H_2O, H_2, and OH.

7) Carbon reaction was limited to the apparent surface of the particle. The effects of pores (causing reaction within the particle), intrinsic variations of carbon black reactivity, and catalysts were treated by introducing empirical area/reactivity multiplication factors of the basic carbon reaction rate.

8) Two surface reaction models were examined, both of which attempt to predict reaction rates over the full range of equivalence ratios where agglomerate reaction rates are significant. The first method employed an approach suggested by Neoh et al.,[15] where carbon reaction with OH is assumed to dominate at high equivalence ratios, while reaction with O_2 becomes more significant at low equivalence ratios. The second procedure followed Libby and Blake[13] for reaction of carbon with oxygen and carbon dioxide, but was extended to include an additional contribution due to reaction of carbon with water vapor.

9) The gas phase was assumed to be in thermodynamic equilibrium at the particle surface.

10) Since agglomerates reach high temperatures, their radiation to solid surfaces surrounding the flow was considered, assuming an emissivity of unity.

The main distinctions between the present analysis and that of Libby and Blake[13] for carbon particle reaction involves consideration of different reaction mechanisms, allowance for forced convection effects, and the use of empirical area/reactivity multiplication factors to represent effects of pores.

Gas Phase Transport

This portion of the analysis generally follows Libby and Blake,[13] and will only be briefly described. Since binary diffusivities are equal, mass transport is conveniently expressed in terms of element mass fractions. Four elements, C, O, N, and H, and seven species, O_2, N_2, CO, CO_2, H_2O, H_2, OH, appear in the analysis. The element and species mass fractions are related as follows:

$$\tilde{Y}_i = \sum_{j=1}^{7} \mu_{ij} Y_j \qquad i=1,4 \tag{2}$$

where μ_{ij} is the mass fraction of the ith element in the jth species. Given the $\tilde{Y}_i$ at a particular location, Eq. (2) provides four equations to determine the seven unknown Y_i. Three additional equations were obtained from the assumption of thermodynamic equilibrium. The equilibrium relations used were

$$2H_2O \overset{K_{p1}}{\rightleftharpoons} 2H_2 + O_2, \qquad 2H_2O \overset{K_{p2}}{\rightleftharpoons} H_2 + 2OH$$

$$2CO_2 \overset{K_{p3}}{\rightleftharpoons} 2CO + O_2 \tag{3}$$

where the K_{pi} are known functions of temperature.

Conservation of mass indicates that the radial mass flow rate per unit solid angle, $m_c'' r_p^2$, is a constant. The governing equations for conservation of elements and total enthalpy then become[14]:

$$m_c'' r_p^2 \frac{d\tilde{Y}_i}{dr} = \rho D \frac{d}{dr}\left(r^2 \frac{d\tilde{Y}_i}{dr}\right) \qquad i=1,4 \tag{4}$$

$$m_c'' r_p^2 \frac{di}{dr} = \frac{\lambda}{C_p} \frac{d}{dr}\left(r^2 \frac{di}{dr}\right) \tag{5}$$

where

$$i = C_p(T - T_{\text{ref}}) + \sum_{i=1}^{7} Y_i i_{f\text{ref}_i} \tag{6}$$

There is no net mass flux of the elements oxygen, nitrogen, and hydrogen at the particle surface. Furthermore, the net mass flux of carbon at the surface is equal to m_c''. Therefore, the surface boundary conditions for Eqs. (4) and (5) are:

$$r = r_p, \qquad i = i_p$$

$$\rho D\left(\frac{d\tilde{Y}_1}{dr}\right)_p = m_c''(1 - \tilde{Y}_{1p}), \quad \rho D\left(\frac{d\tilde{Y}_i}{dr}\right)_p = m_c'' \tilde{Y}_{ip} \quad i=2,4 \tag{7}$$

denoting carbon as species 1. The ambient boundary conditons are:

$$r = r_{\infty_T}, \; i = i_\infty, \; T = T_\infty; \quad r = r_\infty, \; \tilde{Y}_i = \tilde{Y}_{i_\infty}, \; i=1,4 \tag{8}$$

Equations (8) treat the general case where the film radii for mass and heat transfer are not the same. These radii are found from the usual correlations of film theory, as follows[8]:

$$r_{\infty_T}/r_p = Nu/(Nu-2), \qquad r_\infty/r_p = Sh/(Sh-2) \tag{9}$$

Ordinarily, Nu and Sh appearing in Eq. (9) would be obtained from the following correlation:

$$Nu' \text{ or } Sh' = 2 + [0.552 Re^{1/2} (Pr \text{ or } Sc)^{1/3}] / [1 + 1.232/(Re(Pr \text{ or } Sc)^{4/3})]^{1/2} \tag{10}$$

where

$$Re = d_p u_\infty / \nu \tag{11}$$

Equation (10) was developed from theoretical and experimental results for smooth spheres and drops and provided a good correlation of convective effects for drops during this and earlier investigations.[7-11] The use of this equation, however, underestimated transport rates of the present agglomerates for all reasonable selections of physical properties. This behavior was attributed to the fact that the agglomerates have an open porous structure near the surface providing roughness effects and allowing the flow to penetrate the apparent surface to some extent. It was found that this enhancement of convective transport rates could be accommodated in the model by multiplying the Nusselt and Sherwood numbers given by Eq. (10) by a constant convective enhancement factor, $\zeta = 6.7$, as follows:

$$Nu \text{ or } Sh = \zeta(Nu' \text{ or } Sh') \tag{12}$$

over the entire test range. Pending extension of the model to explicitly consider the properties of agglomerate surface structure, this artifice was employed in the following computations so that progress could be made in evaluating the carbon reaction mechanisms for the range of conditions of interest in the analysis of combustion chambers.

The solution of Eq. (4), subject to the boundary conditions of Eqs. (7) and (8), yields:

$$\tilde{Y}_{l_p} = 1 - (1 - \tilde{Y}_{l_\infty}) \exp(-2K/Sh) \tag{13}$$

$$\tilde{Y}_{i_p} = \tilde{Y}_{i_\infty} \exp(-2K/Sh) \qquad i = 2,4 \tag{14}$$

where

$$K = m_c'' r_p / \rho D \tag{15}$$

Employing the sign convention that convection heat transfer from the surface of the particle is positive, we have

$$q_c'' = -\lambda \left(\frac{dT}{dr}\right)_p = -\frac{\lambda}{C_p}\left(\frac{di}{dr}\right)_p \tag{16}$$

where the second part of Eq. (16) follows by neglecting the slight departure of the Lewis number from unity. The solution of Eq. (5) yields the convective heat flux as follows:

$$\frac{q_c'' C_p}{(i_p - i_\infty)} = \frac{\lambda K / r_p}{1 - \exp(2K/LeNu)} \tag{17}$$

Given the ambient conditions, the temperature of the particle, and K, Eqs. (2), (3), (13), (14), and (17) provide the $\tilde{Y}_{i_p}$, Y_{i_p}, and q_c''. The relationship between K and the Y_i required to complete the solution is discussed next.

Surface Reactions

There are numerous uncertainties in modeling the reaction of a porous carbon agglomerate in a flame. The flame environment contains several species that are potential oxidants of carbon, e.g., H_2O, CO_2, O, O_2, and OH, and the reaction mechanism is not well established.[15] Since the material is porous, reaction is not limited to the apparent outer surface of the agglomerate.[16] Carbon substances exhibit intrinsic variations in reactivity due to their surface structure.[16] Finally, the presence of a catalyst was found to influence reaction rates.

The effect of various gaseous reactants was treated by considering a mechanism recently proposed by Neoh et al.,[15] as well as an extension of an earlier approach employed by Libby and Blake.[13] The effect of pores, surface reactivity, and catalyst was treated by identifying empirical area/reactivity factors selected to best match the present measurements. (It was found that a fixed value, for a given carbon black and reaction, could correlate the measurements over the range of the data.)

Neoh et al.[15] concluded that OH is the dominant carbon oxidant under fuel-rich conditions; that O is of secondary importance at temperatures below 2000 K; and that O_2 becomes a significant factor for fuel-lean conditions, particularly at lower temperatures. Present test conditions correspond to these circumstances; therefore, carbon reaction with OH and O_2 was considered, while ignoring the remaining species. Neoh et al.[15] found that reaction of carbon with OH could be represented by assuming a constant collision efficiency, yielding the following reaction rate expression

$$R_1 = K_{r1} p_{OH} \tag{18}$$

The results of Nagle and Strickland-Constable[17] were employed to determine the rate of reaction of carbon with O_2. These rate expressions are also in reasonable agreement with later measurements by Park and Appleton.[18] The carbon reaction rate is given by

$$R_2 = K_{r2} p_{O_2} \chi / (1 + K_{r3} p_{O_2}) + K_{r4} p_{O_2} (1 - \chi) \tag{19}$$

where

$$\chi = [1 + K_{r5} / (K_{r4} p_{O_2})]^{-1} \tag{20}$$

The measurements of Neoh et al.[15] suggest that the larger of R_1 or R_2 should represent the reaction rate at any condition. Therefore, the dimensionless mass burning rate was determined from

$$K = (r_p / \rho D) \max(a_1 R_1, a_2 R_2) \tag{21}$$

where the a_i appearing in Eq. (21) are the empirical area/reactivity multiplication factors.

The carbon reaction mechanism used by Libby and Blake[13] considers reaction with O_2 and CO_2, employing the following expressions

$$R_3 = K_{r6} p_{O_2} \tag{22}$$

$$R_4 = K_{r7} p_{CO_2} \tag{23}$$

Table 2 Summary of reaction rate parameters

i	A	n	E, kcal/gmol
1[a]	361 kg $K^{1/2}/m^2$ s atm	−1/2	0
2	2400 kg/m^2 s atm	0	30.0
3	21.3 atm^{-1}	0	− 4.1
4	0.535 kg/m^2 s atm	0	15.2
5	18.1×10^6 kg/m^2 s	0	97.0
6	87,100 kg/m^2 s atm	0	35.8
7	2470 kg/m^2 s atm	0	41.9
8[b]	15.15×10^{-3} kg/m^2 s atm	0	32.7
9	9.42×10^{-11} atm^{-1}	0	−60.8
10	7.07×10^{-16} atm^{-1}	0	−79.3

[a] Assuming a collision efficiency of 0.28.[15] [b] Assuming a surface area of reaction of 1.15 m^2/g of carbon, which is the average surface area over the period of reaction.[19]

Table 3 Summary of area/reactivity factors

Reaction	Noncatalyzed	Catalyzed
Neoh et al.[15] reaction approximation:		
1	54.3	—
2	758	—
Extended Libby-Blake[13] reaction approximation:		
3	58.2	70.6
4	112.9	140.0
5	112.9	140.0

This approach was extended during the present study to include the reaction of carbon with H_2O, employing the results of Johnstone et al.[19] The reaction rate expression in this case is

$$R_5 = K_{r8} p_{H_2O} / (1 + K_{r9} p_{H_2} + K_{r10} p_{H_2O}) \quad (24)$$

For this second approach, the total reaction rate of carbon was obtained as the sum of the rates for O_2, CO_2, and H_2O, ignoring potential interactions between reactants. This yields

$$K = (r_p/\rho D) \sum_{i=3}^{5} a_i R_i \quad (25)$$

The specific reaction-rate parameters used in the computations are summarized in Table 2, where the K_{ri} are assumed to have the following general form:

$$K_{ri} = A_i T^{n_i} \exp(-E_i/RT) \quad (26)$$

In all cases, p_i was found from the mass fractions at the particle surface as follows:

$$p_i = MY_i p/M_i \quad (27)$$

The area/reactivity factors which provided the best match of the present data are summarized in Table 3. Neoh et al.[15] estimate collision efficiencies for OH in the 0.13-0.28 range, the latter value was employed for the present estimate of a_i. The area/reactivity factors for R_4 and R_5 could not be separated for present test conditions, since the relative proportions of CO_2 and H_2O were roughly the same throughout the flame. Therefore, the values were taken to be identical for both reactions. As might be expected, the presence of pores in the agglomerate result in a_i values greater than unity, since the actual reaction area is greater than the apparent surface area. The a_i for a catalyzed slurry were only evaluated for the second reaction approximation. The use of a catalyst increases the intrinsic surface reactivity of the carbon, yielding higher a_i than for the noncatalyzed agglomerate.

Given the gas phase solution for a specific value of K, the Y_{ip} are found as described earlier. Equations (18-21) for the Neoh et al.[15] approximation, or Eqs. (22-25) for the extended Libby and Blake[13] approximation, yield a prediction for K, allowing an iterative solution for particle transport rates. The computation of average gas phase properties was the same as the liquid gasification computations.

Agglomerate Life History Computation

Given the temperature and size of the particle and the ambient conditions, the gas phase and surface reaction analyses yield the $\tilde{Y}_{i_p}$, Y_{i_p}, K, and q_c''. The variation of the size and temperature of the particle was determined by solving equations for conservation of particle mass and energy.

Assuming that the density of the particle is a constant, conservation of particle mass yields:

$$dr_p/dt = -\rho DK/\rho_c r_p \quad (28)$$

Conservation of energy at the particle surface yields:

$$\frac{dT_p}{dt} = \left(\frac{-3}{\rho_c C_{p_c} r_p}\right)(m_p''(i_p - i_c) + q_c'' + q_r'') \quad (29)$$

where q_r'' is the particle surface heat flux for radiation to the enclosure surrounding the flow:

$$q_r'' = \sigma\epsilon(T_p^4 - T_w^4) \quad (30)$$

The initial conditions for Eqs. (28) and (29) were based on conditions at the end of the liquid vaporization period. At this point, all the carbon initially in the slurry was present in the agglomerate, the agglomerate density is known,[2] and the particle was at the wet-bulb temperature for liquid evaporation.

Equations (28) and (29) were numerically integrated using Gear's method. The nonlinear algebraic set of equations, which must be satisfied in order to determine the $\tilde{Y}_{i_p}$, Y_{i_p}, q_c'' and K, was solved using the Newton-Raphson method, given the current values of T_p, r_p and the ambient conditions.

Agglomerate Burning Rate Results

General Observations

Significant agglomerate reaction rates were only observed for a limited region of thi flame. For present tests along the centerline of a diffusion flame in still air, reaction of noncatalyzed agglomerates was limited to equivalence ratios in the range 0.37 to 1.4, corresponding to $160 < x/d < 400$. The higher surface reactivity of the catalyzed agglomerate yielded a lower lean limit, with reaction observed for equivalence ratios in the range 0.21 to 1.4, corresponding to $160 < x/d < 500$. The range of conditions used to evaluate the agglomerate burning rate theory (see Table 1) roughly spans the region where significant agglomerate reaction was observed.

Figure 1 is a scanning electron microscope photograph of the surface of a partially reacted agglomerate. The light areas on the photograph represent the surface of the solid agglomerate, the dark areas represent pores. While this photograph was for a catalyzed slurry, near the downstream end of the region where reaction was observed, it is generally representative of the appearance of the surface of both catalyzed and noncatalyzed agglomerates at locations where carbon reaction occurred. The agglomerate is clearly very porous, with the carbon surface area available for reaction much greater than the apparent outer surface area of the agglomerate. Furthermore, the open structure clearly could allow the flow to penetrate the apparent surface, contributing to the convective enhancement discussed earlier.

Predicted and measured burning rates for noncatalyzed agglomerates are illustrated in Figs. 2 and 3. Burning rate is plotted as a function of agglomerate diameter with position in the flame (equivalence ratio) as a parameter. The predictions employ the reaction parameters summarized in Tables 2 and 3, as well as the convection enhancement factor. For this selection of parameters, the two reaction approximations give nearly the same results, and both methods can be represented by a single line. Clearly, the use of this fixed set of parameters provides a good representation of the data over the entire range of the tests. The low reaction rates at low equivalence ratios were also predicted reasonably well, suggesting that the

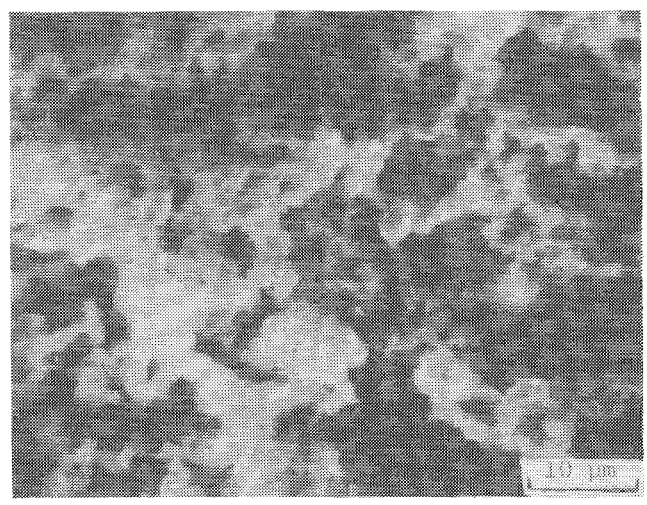

Fig. 1 SEM photograph of the surface of catalyzed agglomerate after quenching at $x/d = 489$.

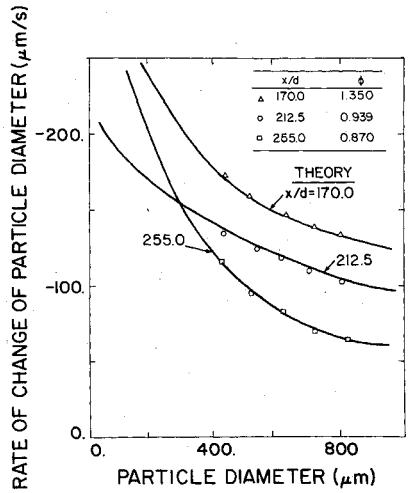

Fig. 2 Quasisteady burning rates for noncatalyzed agglomerates at high equivalence ratios.

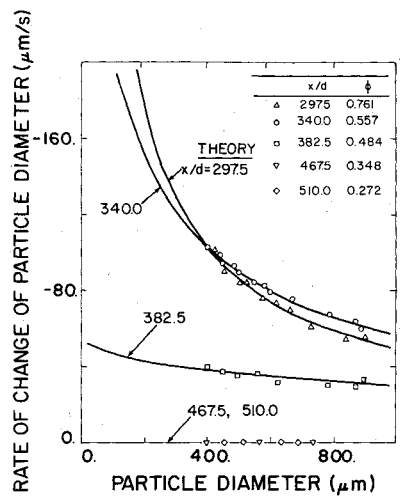

Fig. 3 Quasisteady burning rates for noncatalyzed agglomerates at low equivalence ratios.

model has some potential for predicting the quenching of the agglomerate reaction.

There are two main combustion limits for carbon agglomerates—the reaction-controlled limit and the diffusion-controlled limit.[16] For the reaction-controlled limit, reaction rates are low in comparison to diffusion rates, and there is no mass transfer limitation on the supply of gaseous reactants to the particle surface. This limit is characterized by the burning rate being relatively independent of particle diameter, e.g., results for $x/d \geq 382.5$ in Fig. 3 approach the reaction-controlled limit.

The diffusion-controlled limit is characterized by high reaction rates in comparison to diffusion rates, leading to small concentrations of reactant gases at the particle surface. In this case, the burning rate is largely determined by the mass transfer properties of the flow around the particle. The magnitude of the burning rate is then influenced by particle diameter as follows:

$$-\frac{dd_p}{dt} \sim d_p^{-(0.5-1)} \tag{31}$$

The power of d_p in Eq. (31) tends toward -1 as the Reynolds number of the particle decreases. From this argument, it is apparent that results in the $255.0 \leq x/d \leq 340$ range, in Figs. 2 and 3, are approaching the diffusion-controlled limit. The remainder of the measurements involve both reaction and

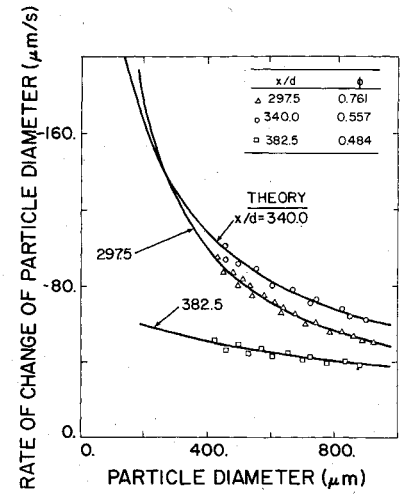

Fig. 4 Quasisteady burning rates for catalyzed agglomerates.

diffusion effects to some extent. Diffusion rates become large for small particles; therefore, all regions of the flow would eventually exhibit reaction rate control for sufficiently small particles.

Figure 4 is an illustration of predicted and measured burning rates for the catalyzed agglomerate. These test results were limited to $x/d = 297.5$, 340.0, and 382.5, while the analysis was limited to extended Libby-Blake[13] reaction mechanisms. Consumption of the agglomerate is nearly diffusion controlled at the first two positions, resulting in little change in the burning rate when the catalyst was used. At $x/d = 382.5$, however, adding catalyst increased the burning rate 20-25%, since agglomerate consumption is nearly reaction rate controlled at this position. Naturally, the effect of catalyst is greater at positions farther downstream, e.g., the presence of catalyst reduced the lean limit for quenching from an equivalence ratio of 0.37 to 0.21.

Another property of catalyzed slurries was their tendency to spontaneously shatter from time to time. When observed, shattering occurred after all the liquid had apparently evaporated. This behavior could be influenced by the presence of the drop support, and was not consistently observed. If shattering does persist for small, unsupported particles, however, this would provide another (physical) mechanism for the improved combustion properties observed for catalyzed slurries during combustion chamber tests.[2,3] Tests with unsupported particles, having sizes more typical of sprays, will be required in order to establish the importance of this effect.

Slurry Drop Life Histories

The final step in evaluating the model involved comparison of predicted and measured slurry drop life histories. Life histories were computed for noncatalyzed slurries over the test range. A portion of the results are illustrated in Figs. 5-7, which covers equivalence ratios of 0.348-1.350. Predicted and measured particle diameters and temperatures are plotted as a function of time, with results illustrated for both reaction approximations. For reference purposes, the local temperature of the flow is also shown on each plot. The time scale of each figure has been expanded in the period where liquid is present, since this period is short in comparison to the total lifetime of the slurry drop.

The two-stage combustion process of slurry drops is quite evident from the results pictured in Figs. 5-7. The first stage involves heat-up of the particle to the wet-bulb temperature for liquid gasification. Some evaporation occurs throughout this period; however, the rate is highest when the particle is near the wet-bulb temperature. Since JP-10 is a pure hydrocarbon, its wet-bulb temperature is nearly constant at a fixed location in the flame (having a value somewhat below

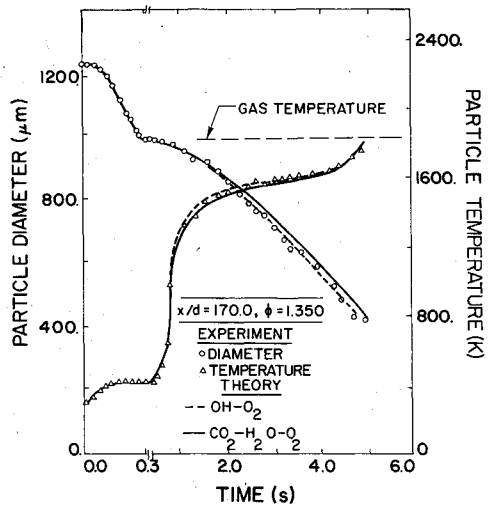

Fig. 5 Noncatalyzed slurry drop life history at $x/d = 170.0$.

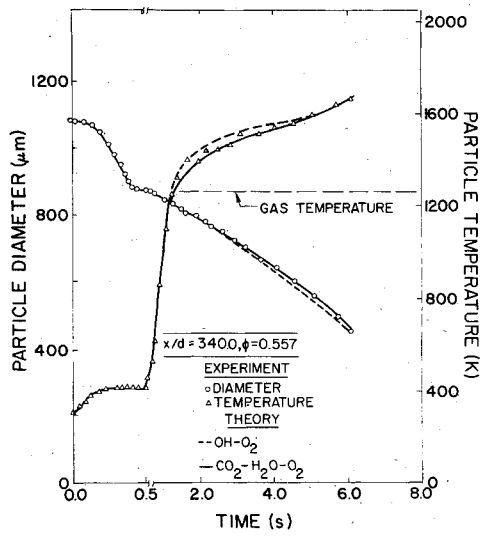

Fig. 6 Noncatalyzed slurry drop life history at $x/d = 340.0$.

the boiling temperature of the liquid).[8] The second stage involves heat-up and reaction of the agglomerate, once all the liquid has evaporated. Initially, the variation of agglomerate diameter is relatively slow in this period, until the particle temperature approaches the gas temperature. Maximum particle temperatures can be above or below the gas temperature, depending on the energy release by reaction, and heat transport by convection and radiation. Near the lean and rich limits, particle temperatures tend to be below the flame temperature, due to radiative heat losses. Intermediate equivalence ratios, e.g., 0.557 for Fig. 6, yield relatively high reaction rates and particle temperatures exceed the flame temperature. The relative rates of reaction, convection, and radiation, however, vary with particle size. Therefore, there is no fixed particle temperature during the latter part of agglomerate reaction, even at a fixed location in the flame, unlike the liquid evaporation period. As the particle becomes small, however, convection heat-transfer rates become large in comparison to reaction and radiation effects, and the particle eventually approaches the local gas temperature. This is not observed in Figs. 5-7 due to the finite-sized bead used to mount the slurry drop.

The comparison between the predictions and measurements illustrated in Figs. 5-7 is quite good. This is partly expected, since the model was capable of correlating the burning rate measurements for this range of flame conditions. However, it is encouraging that the model is also capable of predicting

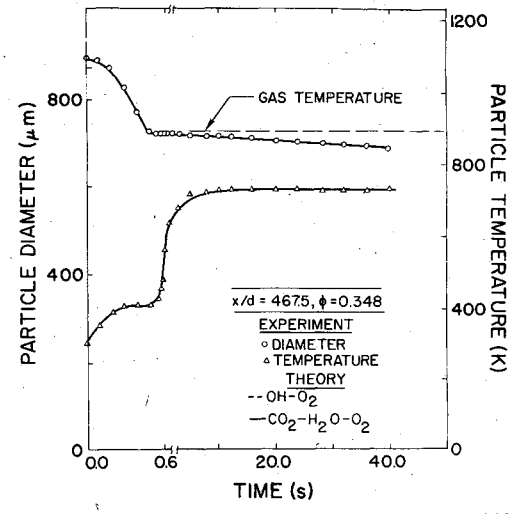

Fig. 7 Noncatalyzed slurry drop life history at $x/d = 467.5$.

heat-up, where reaction effects are small, as well as final temperature levels, where radiation becomes important. There is little difference in the predictions using the two reaction approximations, similar to the agglomerate burning rate results.

Conclusions

The present measurements showed that all the solid carbon in the slurry remained to form an agglomerate and that heat-up and reaction of the agglomerate required the bulk of the lifetime of the particle (90-95% even in locations where agglomerate reaction rates were maximum). Adding catalyst increased agglomerate reaction rates, except at the diffusion-controlled conditions, and also extended the lean limit for quenching, e.g., agglomerate reaction was observed for flame equivalence ratios of 0.37-1.4 for noncatalyzed agglomerates and 0.21-1.4 for catalyzed agglomerates. Agglomerate shattering was occasionally observed with catalyzed slurries at low equivalence ratios.

The model developed here provided a good correlation of agglomerate reaction rates and life histories, using either the Neoh et al.,[15] or extended Libby-Blake[13] reaction mechanisms, over the complete equivalence ratio range where appreciable agglomerate reaction was observed. While this was encouraging, effects of pressure, different C/H ratios of the flame gases, and different temperature levels for given equivalence ratios (due to air preheat) still must be assessed.

The present model employs an oversimplified treatment of agglomerate structure, involving the assumption of a smooth surface with empirical convection enhancement and area/reactivity factors to allow for effects of flow penetrating the porous surface, pore diffusion, intrinsic surface reactivity, and catalyst. These empirical factors were found to be constants over the present test range (400-1000 μm diam particles at atmospheric pressure). The constants were significantly greater than unity, suggesting that the open, porous structure of the agglomerate strongly influences the reaction process. Since effects of surface structure probably vary with particle size, properties of the carbon black, and flow conditions, it is unlikely that the empirical factors found in the present study are generally appropriate. Work is continuing in this laboratory in order to examine the variation of the empirical factors over a broader range of test conditions, particularly emphasizing smaller particles more representative of practical slurry sprays, pending development of a more complete model of the agglomerate structure.

The liquid gasification portion of the slurry drop lifetime was relatively conventional. Use of the existing methods for predicting liquid drop life histories,[7-11] yielded good results during the present investigation.

Acknowledgment

This research was supported in part by the Office of Naval Research, Contract N00014-80-C-0517, the Air Force Aero Propulsion Laboratory, Contract F33615-77-C-2004, and the AiResearch Manufacturing Company of Arizona. Test fuels were provided by R. S. Stearns of Suntech Group.

References

[1] Burdette, G. W., Lander, H. R., and McCoy, J. R., "High Energy Density Fuels for Cruise Missiles," AIAA Paper 78-267, Jan. 1978.

[2] Bruce, T. W., Mongia, H. C., Stearns, R. S., Hall, L. W., and Faeth, G. M., "Formulation Properties and Combustion of Carbon-Slurry Fuels," *Proceedings of Sixteenth JANNAF Combustion Meeting,* CPIA Pub. No. 308, 1979, pp. 679-717.

[3] Bruce, T. W. and Mongia, H., "Compound Cycle Turbofan Engine Task IX: Carbon-Slurry Fuel Combustion Evaluation Program," AFWAL-TR-80-2-35, March 1980.

[4] Salvesen, R. H., "Carbon Slurry Fuels for Volume Limited Missiles," AFAPL-TR-79-2122, Nov. 1979.

[5] Miyasaka, K. and Law, C. K., "Combustion and Agglomeration of Coal-Oil Mixtures in Furnace Environments," *Combustion Science and Technology,* Vol. 24, Oct. 1980, pp. 71-82.

[6] Law, C. K., Law, H. K., and Lee, C. H., "Combustion Characteristics of Droplets of Coal/Oil and Coal/Oil/Water Mixtures," *Journal of Energy,* Vol. 4, 1979, pp. 329-339.

[7] Mao, C-P., Szekely, G. A. Jr., and Faeth, G. M., "Evaluation of a Locally Homogeneous Flow Model of Spray Combustion," *Journal of Energy,* Vol. 4, March-April 1980, pp. 78-87.

[8] Faeth, G. M., "Current Status of Droplet and Liquid Combustion," *Progress in Energy Combustion Science,* Vol. 3, 1977, pp. 191-224.

[9] Shearer, A. J., Tamura, H., and Faeth, G. M., "Evaluation of a Locally Homogeneous Flow Model of Spray Evaporation," *Journal of Energy,* Vol. 3, Sept.-Oct. 1979, pp. 271-278.

[10] Mao, C-P., Wakamatsu, Y., and Faeth, G. M., "A Simplified Model of High Pressure Spray Combustion," *Eighteenth Symposium (International) on Combustion,* The Combustion Institute, Pittsburgh, Pa., 1981, pp. 337-347.

[11] Faeth, G. M., "Spray Combustion Models—A Review," AIAA Paper 79-0293, Jan. 1979.

[12] Ubhayakar, S. K. and Williams, F. A., "Burning and Extinction of a Laser-Ignited Carbon Particle in Quiescent Mixtures of Oxygen and Nitrogen," *Journal of the Electrochemical Society,* Vol. 123, 1976, pp. 747-756.

[13] Libby, P. A. and Blake, T. R., "Theoretical Study of Burning Carbon Particles," *Combustion and Flame,* Vol. 36, Oct. 1979, pp. 139-169.

[14] Williams, F. A., *Combustion Theory,* 1st ed., Addison-Wesley, Reading, Mass., 1965, Chap. 1.

[15] Neoh, K. G., Howard, J. B., and Sarofim, A. F., "Soot Oxidation in Flames," *Particulate Carbon Formation During Combustion,* edited by D. C. Siegla and G. W. Smith, Plenum Press, New York (in press).

[16] Laurendau, N. M., "Heterogeneous Kinetics of Coal Char Gasification and Combustion," *Progress in Energy Combustion Science,* Vol. 4, 1978, pp. 221-270.

[17] Nagle, J. and Strickland-Constable, R. F., "Oxidation of Carbon Between 1000-2000°C," *Proceedings of Fifth Carbon Conference,* Vol. 1, 1962, pp. 154-164.

[18] Park, C. and Appleton, J. P., "Shock-Tube Measurements of Soot Oxidation Rates," *Combustion and Flame,* Vol. 20, No. 3, June 1973, pp. 369-379.

[19] Johnstone, J. F., Chen, C. Y., and Scott, D. S., "Kinetics of the Steam-Carbon Reaction in Porous Graphite Tubes," *Ind. Engr. Chem.,* Vol. 44, July 1952, pp. 1564-1569.